Field Crops Research 111 (2009) 218–225

Contents lists available at ScienceDirect

Field Crops Research

journal homepage: www.elsevier.com/locate/fcr

A spectral index to monitor the head-emergence of wheat in semi-arid conditions

Agustin Pimstein [a], Jan U.H. Eitel [b], Dan S. Long [c], Israel Mufradi [d], Arnon Karnieli [a], David J. Bonfil [d,*]

[a] The Remote Sensing Laboratory, Jacob Blaustein Institute for Desert Research, Ben Gurion University of the Negev, Sede-Boker Campus 84990, Israel
[b] Geospatial Laboratory for Environmental Dynamics, University of Idaho, Moscow, ID 83843, USA
[c] USDA-ARS, CPCRC, PO Box 370, Pendleton, OR 97810, USA
[d] Field Crops and Natural Resources Department, Agricultural Research Organization, Gilat Research Center, 85280 MP Negev 2, Israel

ARTICLE INFO

Article history:
Received 21 May 2008
Received in revised form 19 December 2008
Accepted 20 December 2008

Keywords:
Zadoks
Vegetation index
Normalized heading index (NHI)
Canopy reflectance
Water status
Advanced land imager (ALI) satellite images
Decision support system (DSS)

ABSTRACT

Harvesting wheat (*Triticium aestivum* L.) for forage or leaving it for grain is the main decision uncertainty growers face in semi-arid regions during mid-season. To facilitate decision-making, a decision support system (DSS) has recently been proposed that requires information about crop water and nutritional status during spike emergence. Though remote sensing has been used to provide site-specific crop status information, a spectral vegetation index is needed to ensure that the information has been acquired during spike emergence. The objective of this study was to propose a spectral index sensitive to spike emergence and validate its suitability across different commercial farm fields by using ground spectral measurements and multispectral satellite imagery. To develop the index, controlled experiments with commonly grown wheat varieties were conducted during the 2004/2005 and 2005/2006 growing season in the agricultural area of the northern Negev desert of Israel. The experiments showed that spike emergence correlated most strongly ($r = 0.7$, $p < 0.05$) with spectral changes near the 1.2 μm water absorption feature in contrast to the band at 1.1 μm which appeared to be only weakly correlated. Thus, the spike emergence sensitive band at 1.2 μm has been combined with the insensitive band at 1.1 μm as reference to form the ratio-based normalized heading index (NHI). Experimental data were then used to establish an index threshold that helps separate data acquired before and after spike emergence. The proposed NHI was able to identify spike emergence with a classification accuracy varying between 53 and 83%. Accuracy was influenced by season, and whether narrow or broad spectral bands were used. Validation of the index in commercial farm fields in Israel and the United States showed that the classification accuracy was similar for ground spectral measurements and the advanced land imager (ALI) satellite imagery. These results suggest that the NHI is suited for identifying the onset of heading throughout wheat-growing areas without the need for characterizing seasonal trends.

1. Introduction

Spatio-temporal data required for site-specific crop management have become increasingly available to growers thanks to the development of new sensors and methodologies. Adoption of this information technology by farmers is expected to increase as appropriate decision support systems become available (McBratney et al., 2005; Eom and Kim, 2006) to translate the acquired data into site-specific management decisions (Arnott and Pervan, 2005). Recently, the heading decision support system (Heading-DSS) was developed for semi-arid conditions in Israel to decide whether to: (i) in case of drought, harvest the crop early for hay or silage, or, (ii) in case of abundant water, harvest for grain at physiological maturity (Bonfil et al., 2004a,b).

To run the Heading-DSS, timely and detailed information on crop water- and nitrogen (N)-status is needed by the end of the booting stage to apply that information into N management during heading. In wheat (*Triticium aestivum* L.), the heading stage is critical because it sets the conditions for the reproductive stage of growth that is reflected in final grain quality and yield (Bonfil et al., 2004a). Remotely sensed data can provide instant information about crop N- (Gitelson et al., 1996; Long et al., 2000; Flowers et al., 2001; Eitel et al., 2007) and water-status (Peñuelas et al., 1993; Gao, 1996; Eitel et al., 2006; Pimstein et al., 2007) over large geographic areas, which can then be used to apply the Heading-DSS for large geographic areas. Therefore, as the Heading-DSS needs to be applied at heading stage of the crop, using remotely sensed images for simultaneously detecting crop canopy condition and its development stage could increase the efficiency of the application of the DSS.

Methods to remotely characterize crop phenology include fitting trigonometric or wavelet functions to time series of

* Corresponding author. Tel.: +972 8 9928654; fax: +972 8 9926485.
E-mail address: bonfil@volcani.agri.gov.il (D.J. Bonfil).

0378-4290/$ – see front matter © 2008 Elsevier B.V. All rights reserved.
doi:10.1016/j.fcr.2008.12.009

vegetation indices that are based on either degree-days (Fischer, 1994; Sakamoto et al., 2005) or days-after-emergence (Fischer, 1994; Sakamoto et al., 2005). These algorithms rely upon vegetation indices and their correlation with leaf area index and biomass. However, changes in biomass are subtle within the reproductive period of growth in wheat (Pal, 1966) and thus one would not expect time-frequency functions to work well for detecting the heading time. In addition, several images are required for matching spectral measurements with a phenologic function thus increasing cost and complexity.

Few studies have explored the suitability of remotely sensed data to detect the appearance of reproductive structures of field crops. Viña et al. (2004) showed that the visible atmospherically resistant index (VARI), employing blue (0.46–0.48 μm), green (0.545–0.565 μm), and red reflectance (0.62–0.67 μm), was able to detect tassel appearance in maize (*Zea mays* L.), but image time series were required for detecting other development stages. At different phenological stages of rice (*Oriza sativa* L.), Kobayashi et al. (2001) studied the effect of panicle blast infection on canopy reflectance throughout the entire optical range (0.4–2.5 μm). They also separately measured reflectance properties of vegetative organs and panicles and showed that canopy reflectance of rice was most strongly affected near 1.2 μm by removal of reproductive structures.

The objectives of this study were to: (1) identify wavelengths most suitable to detect head-emergence in wheat; (2) propose a novel spectral index based on these identified wavelengths and (3) validate the proposed index throughout commercial wheat fields by using ground spectral and satellite data.

2. Materials and methods

This work was based on ground spectral measurements and biophysical analyses of spring wheat canopies. During the 2004/2005 and 2005/2006 growing seasons, controlled field experiments were conducted in Israel at the Gilat Research Center (31°20′6″N, 34°39′6″E at 150 m.a.s.l.). The soil at the research center is a Calcic Xerosol sandy loam loess. The climate is semi-arid and characterized by highly variable interannual rainfall (Bonfil et al., 1999). To validate the newly proposed heading index, data were collected from commercial fields during the 2005/2006 and 2006/2007 growing season.

2.1. Experimental plots

During the 2004/2005 growing season, 11 wheat varieties (Atir, Beit HaShita, Gedera, Galil, Negev, Nirit, Rotem, Shaphir, Shoham, Yuval, and Zahir) were grown to produce different stages of development on a given date. The experiment was a completely randomized design with two replications for each cultivar resulting in a total of 22 plots. Individual plots were approximately 4 m wide and 18 m long. Seeding occurred on 16 November 2004. Row spacing was 20 cm and the seeding rate was 210 pure live seeds m^{-2}. Biophysical and spectral measurements were taken shortly before and during heading [83, 95 and 113 days-after-emergence (DAE)] resulting in a total of 66 samples.

In 2005/2006, only five varieties (Gedera, Galil, Rotem, Yuval, and Zahir) were grown. They were replicated four times (20 total plots) and seeded on mid November 2005 with a density of 210 plants m^{-2} in 10.5 m × 10.0 m plots. Considering that the previous season was relatively wet (334 mm) compared to the mean rainfall (237 mm), the decision was made to apply supplemental irrigation at the beginning of this second season to avoid potential drought stress. Three measurements of biophysical and spectral data were obtained on 71, 86 and 106 DAE, resulting in a total of 57 samples for the 2005/2006 growing season. Complete emergence was registered around the end of November for all varieties and both seasons.

2.2. Biophysical measurements

Zadoks code: The phenological stage of each field or plot was determined according to the Zadoks code for growth stages in cereals (Zadoks et al., 1974). This code is based on ten principal plant development stages starting with germination (Zadoks code 0), and ending with ripening (Zadoks code 9). Each principal development stage can be subdivided into 10 secondary stages and used to clearly identify a given growth stage. The range of growth stages considered during heading in wheat fluctuates from Zadoks 51 (first spiklet of ear just visible) to 69 (anthesis complete).

Biomass development: During the 2005/2006 growing season, crop biomass was characterized by measuring leaf area index (LAI) and dry-weight biomass. LAI measurements were obtained with the AccuPAR Ceptometer LP-80 (Decagon Devices, Inc., Pullman, WA, USA) shortly before reflectance measurements were taken. Biomass was determined by sampling 0.3 m^{-2} (three rows) of the crop from the same locations where the reflectance and LAI measurements had been taken. Dry weight of the biomass was determined upon oven drying at 70 °C for 48 h.

Relative water content: For each biomass sample, the relative water content (RWC) was determined by the fresh weight that was measured within 2 h of sampling and the dry weight upon oven drying at 70 °C for 48 h. The water content corresponds to the difference between the fresh weight and the dry-weight biomass.

2.3. Spectral data

Canopy radiance was measured at solar noon ±1 h under cloud-free conditions with a Field Spec® Pro spectrometer (Analytical Spectral Devices, Boulder, CO, USA). The spectrometer is sensitive to the 0.35–2.50 μm spectral range and its fiber optic probe has a 25° field of view. The measurements were collected pointing towards nadir approximately 0.9 m above the canopy. Spectral reflectance was obtained after periodic radiance measurements, using a Spectralon standard white reference panel (Labsphere, Inc., North Sutton, NH, USA). The spectrometer was programmed to automatically calculate the average of 20 readings that were taken at each sampling point. The spectral regions 1.35–1.42 and 1.80–1.96 μm were eliminated from the analysis because they are strongly affected by atmospheric water absorption. Because the spectrometer consists of three sensors with spectral resolutions of 3 and 10 nm, the data were interpolated linearly to 5 nm narrow bands. Spectral data were resampled to band equivalence reflectance (BER) of the advanced land imager (ALI) based on the procedure outlined in Eitel et al. (2007).

2.4. Structuring the heading index

A novel heading index was developed based upon the widely employed rationing concept of two bands: namely, an index and reference band (Rollin and Milton, 1998; Pu et al., 2003; Eitel et al., 2006). The index band varies with the variable of interest (in this study plant phenological changes during heading) as opposed to the reference band which is relatively unaffected by the latter (Sims and Gamon, 2003). Thus, with plant physiological changes caused by heading, the index band would change in relation to the reference band and thus their ratio. The ratioing of two bands also helps to reduce external variation caused by viewing and illumination geometry as well as canopy background variation (Jensen, 2000). The specific bands considered for the ratio or

spectral index had to fulfill the following requirements to ensure that index variations are mostly caused by variations in Zadoks:

(i) The index had to contain a band that is strongly correlated to Zadoks and a reference band that is weakly correlated to Zadoks.
(ii) Both bands have to be similarly affected by changes in biophysical properties (e.g. dry mass, crop water status, crop nutrient status), and need to have similar soil reflectance.

2.5. Index validation

For the resulting index, a threshold was determined based on the experimental data that best separate samples acquired before and after heading (Zadoks = 60). The defined threshold was validated across different commercial farm fields and two growing seasons (2005/2006 and 2006/2007). The accuracy was measured by calculating an overall error of the samples that were not correctly classified (before or after heading) for each of the experimental datasets.

2.5.1. Ground spectral measurements

Ground spectral measurements were obtained in commercial wheat fields near the Gilat Research Center in Israel (Kibbutz Saad 31°28′15″N, 34°32′5″E and Kibbutz Mishmar HaNegev 31°20′39″N, 34°41′8″E) and near Helix, Oregon in the United States (45°48′54″N, 118°40′51″W). The growing and climate conditions of the Israeli fields are similar to those described for the experimental plots above. The United States study site is characterized by silt loam soils, annual precipitation that varies between 300 and 380 mm, and average annual air temperature of 10–12°C. In Israel, 85 commercial farm fields were selected during the 2005/2006 growing season, and 48 during the 2006/2007 growing season. In the United States, 52 plots were placed within a single commercial farm field during the 2006 growing season. The wheat in this field was highly variable in phenology stages. Zadoks code was determined for each field, and ground spectral measurements were acquired according to the procedure described in Section 2.3.

2.5.2. Satellite level measurements

One ALI image of the northern Negev was collected during the heading stage of the 2006/2007 growing season (25 February 2007), and compared to the growth stages from 158 fields that were examined close to the image acquisition date. ALI is a multispectral sensor, on the EO-1 satellite that follows a sun-synchronous, near-polar orbit with a nominal altitude of 705 km at the equator, collecting images with an approximate 100 by 50 km footprint. The ALI sensor acquires 30-m data in 10 broad (>10 nm)-bands. In addition to bands measured by the Landsat MS sensor, it has three additional bands at 0.433–0.453, 0.845–0.890 and 1.200–1.300 μm. One panchromatic band is available at a spatial resolution of 10 m.

The software package ERDAS Imagine (Erdas, Inc.) was used for image pre-processing. The dark object subtraction method (Chavez, 1996) was used to perform atmospheric correction of the imagery. Image-to-image registration was carried out by registering each image to an orthoimage. Subsequently, study sites within the image scene were delineated using ArcView (Environmental Systems Research Institute, Inc.). Areas within fields, which differed in terms of crop developmental stage, were considered as different fields.

3. Results and discussion

3.1. Spectral and biophysical changes in wheat during heading

Wheat developed faster in the 2005/2006 growing season than during the 2004/2005 growing season because of relatively lower precipitation, higher mean air temperature, and higher minimum soil temperature (data not shown). During the 2004/2005 growing season, flag leaf and spike emergence were observed 83 DAE (Zadoks code between 38 and 59). In comparison, more advanced stages of development were already observed at 71 DAE (Zadoks code between 44 and 71) during the 2005/2006 growing season. However, crop development slowed later in the growing season, reaching the beginning of dough development (Zadoks code 80) at around 110 DAE, similar to what was observed during the 2004/2005 growing season.

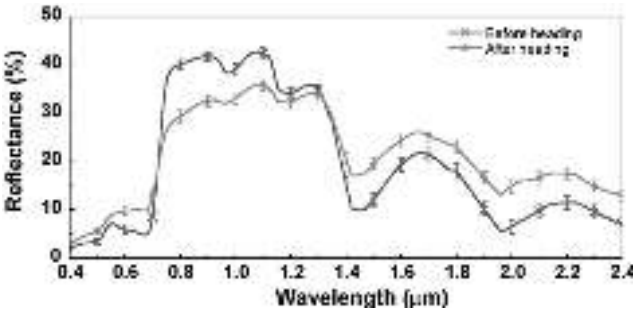

Fig. 1. Average reflectance of data collected before and after heading. Each error bar represents one standard deviation.

By monitoring the wheat condition throughout the late stages of the season, it was possible to register spectral changes associated with heading. As the fields had already reached full canopy coverage, these changes were characterized by a strong reduction in near infrared (NIR) reflectance (0.75–1.10 μm) and little change in SWIR reflectance between 1.1 and 1.3 μm. NIR reflectance before and after heading differs significantly vs. SWIR which has nearly same reflectance (Fig. 1). These differences form the foundation for the proposed heading index.

Monitoring biomass and plant water content facilitated the understanding of the differences observed in the crop spectrum. Biomass increased linearly from 430 to approximately 1000 g m^{-2} during the 2005/2006 growing season (data not shown). After almost no change during the season, RWC started to decrease towards heading thus agreeing with previous observations (Bonfil et al., 2004a; Pimstein et al., 2007).

The decrease of NIR-SWIR reflectance with increasing biomass contradicts what has been largely reported for NIR reflectance, i.e., that it increases with an increase in biomass (Jensen, 2000; Lillesand and Kiefer, 2000). However, if the absolute water content (DW × RWC) in the canopy is considered, instead of the RWC, its increase explains the decrease of NIR-SWIR reflectance. This agrees with findings by Haboudane et al. (2004) who observed that NIR reflectance decreased during the heading stage, mimicking the

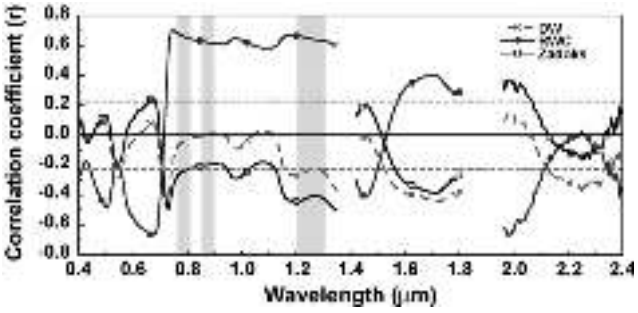

Fig. 2. Correlation coefficients between biophysical parameters (dry weight (DW), RWC and Zadoks code) and reflectance. Gray bars indicate the ALI bands #5, #6 and #7; horizontal red dashed lines indicate significance level ($p < 0.05$). (For interpretation of the references to color in this figure legend, the reader is referred to the web version of the article.)

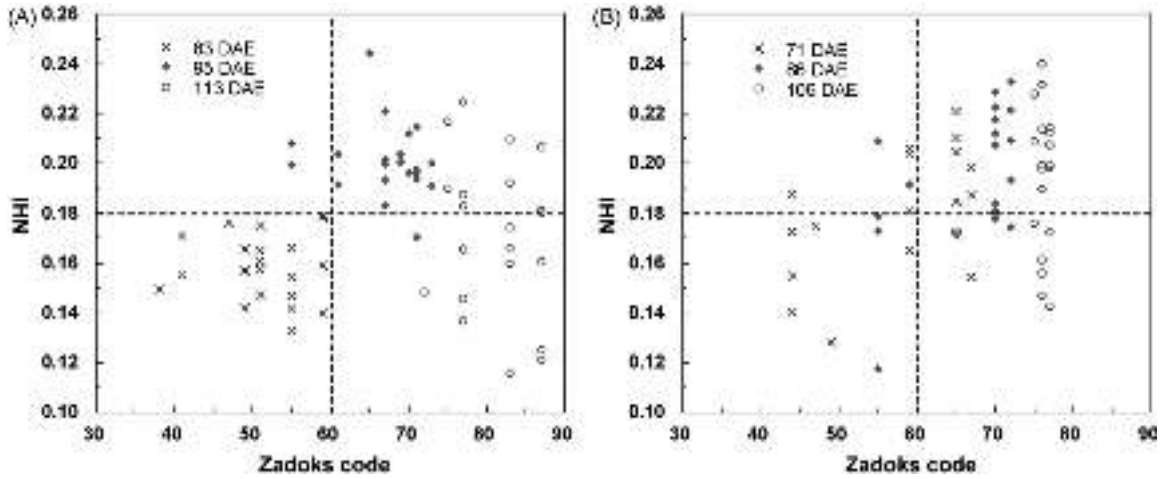

Fig. 3. Scatterplots of NHI vs. Zadoks code using narrow band spectral measurements. (A) 2004/2005 growing season; (B) 2005/2006 growing season. Dotted lines indicate the NHI and Zadoks thresholds.

spectral response of a reduction in biomass. The fact that the LAI did not change significantly between the last two measurements (average of 4.4 for 20 February 2006 and 4.1 for 12 March 2006), indicates that the increase of biomass after heading was mostly due to grain filling and stem enlargement (Salisbury and Ross, 1994; Acevedo et al., 2002).

As there was only a slight difference in the most visible reflectance (0.40–0.55 μm) before and after heading (Fig. 1), the importance of the NIR-SWIR range for monitoring RWC, DW, and phenological stage under high biomass conditions is stressed. This is confirmed in Fig. 2, showing the correlation coefficients (r) between the reflectance at each wavelength and each of the three variables. Observed NIR-SWIR reflectance changes are explained mainly by the changes in RWC (correlation coefficient ~0.65) (Fig. 2). This coincides with previous work at both leaf and canopy levels that specifically showed increasing difference in reflectance between 1.0 and 1.2 μm that is associated with water content (Rollin and Milton, 1998; Zarco-Tejada et al., 2003). In addition, Zadoks code was significantly correlated with reflectance within the following ranges of wavelengths: 0.72–0.80, 0.95–1.00, 1.13–1.35, 1.57–1.80, and 1.96–2.07 μm.

3.2. Development of a heading index

Reflectance measured at 0.75 and 1.20 μm showed the strongest correlation to Zadoks code and thus considered for use as index wavelengths (Fig. 2). Other wavelengths located in the visible domain showed no or only weaker relationships to Zadoks code and thus is considered for use as an index wavelength. However, since their sensitivity to variations in RWC and DW differ from those shown for potential index wavelengths at 0.75 and 1.20 μm, i.e. they violate requirement (ii) listed in Section 2.4, and thus were not considered. Instead, the wavelength located at 1.1 μm was selected as the reference wavelength because it was unrelated to Zadoks code and was similarly affected by variations in RWC and DW as wavelengths at 0.75 and 1.2 μm. Finally, the wavelength at 1.2 μm was selected over the wavelength at 0.75 μm as the reference wavelength since the effects of variation in RWC and DW are more similar to those shown for the reference wavelength at 1.1 μm. In addition, the wavelengths centered at 1.1 and 1.2 μm fulfill the requirement of similar soil reflectance that fluctuates within 2% and 5% of their reflectance values in semi-arid to arid soils in Israel (Malley et al., 2004). Thus, the newly proposed normalized heading index (NHI) was written as follows:

$$\mathrm{NHI} = \frac{\rho_{1.1} - \rho_{1.2}}{\rho_{1.1} + \rho_{1.2}} \quad (1)$$

where ρ represents the reflectance at the respective wavelengths in μm.

Based on the previously described experiments, it was determined that NHI values <0.18 were mostly associated with wheat plants before heading (Zadoks < 60), and NHI values >0.18 with wheat plants that had passed heading (Zadoks ≥ 60) (Fig. 3). This 0.18 threshold misclassified 21% of the 2004/2005 season samples and 32% of the 2005/2006 season (Table 1A). Specifically, most of the error resulted from samples that were classified as *before heading* (BH) when they belonged to the *after heading* (AH) class (Table 1B). These late-season samples had biomass similar to that of the previous dates, but their NDVI decreased from 0.9 in most samples to lower values. For this reason, NHI was divided by NDVI to make NHI more sensitive to late-season changes. This new version of the index is termed the corrected normalized spectral heading index (NHIc, Eq. (2)) and is useful for fields where senescence has started.

$$\mathrm{NHIc} = \frac{(\rho_{1.1} - \rho_{1.2})/(\rho_{1.1} + \rho_{1.2})}{(\rho_{0.85} - \rho_{0.67})/(\rho_{0.85} + \rho_{0.67})} \quad (2)$$

As can be seen in Fig. 4, the correction of NHI by NDVI, increased the previously determined threshold value from 0.18 to 0.20. As a result, misclassification decreased from 21 to 17% during the 2004/

Table 1A
Thresholds and prediction error of NHI and NHIc calculated with narrow and broadband data (ALI resampling based on ASD measurements) on experimental plots and commercial fields.

	Samples no.	Narrow NHI	Narrow NHIc	Broad NHI (ALI-BER)	Broad NHIc (ALI-BER)
Threshold		*0.18*	*0.20*	*0.18*	*0.20*
Experimental plots 2004/2005	66	21%	17%	36%	33%
Experimental plots 2005/2006	57	32%	25%	40%	32%
Commercial fields 2005/2006	87	30%	28%	47%	44%
Commercial fields 2006/2007	48	23%	23%	23%	23%

Table 1B
Confusion matrix between registered and classified phenological stage for the different datasets and heading indices. BH: before heading (Zadoks < 60); AH: after heading (Zadoks ≥ 60). Diagonal italic numbers correspond to the correct classification.

	Predicted	Narrow NHI		Narrow NHIc		Broad NHI (ALI-BER)		Broad NHIc (ALI-BER)	
Observed		BH	AH	BH	AH	BH	AH	BH	AH
Experimental plots 2004/2005	BH	*22*	2	22	2	20	4	21	3
	AH	12	*30*	9	33	20	22	19	23
Experimental plots 2005/2006	BH	9	6	*10*	5	7	8	9	6
	AH	12	30	9	*33*	15	27	12	30
Commercial fields 2005/2006	BH	45	10	45	10	*32*	23	34	21
	AH	16	16	14	18	18	*14*	17	15
Commercial fields 2006/2007	BH	16	4	16	4	15	5	*15*	5
	AH	7	21	7	21	6	22	6	*22*

2005 growing season and from 32 to 25% in the 2005/2006 growing season (Table 1A). As expected, this increase in accuracy is given by better classifications of the samples that were AH (Table 1B). The accuracy of the prediction of the samples that were BH was improved by only one sample.

Though NHIc provided better results for both seasons, this was only true if senescing samples (DAE > 106) were included in the analysis. When senescing samples were removed from the analysis, the NHI performed better than NHIc, confirming that normalizing the original NHI index by the biomass condition (NDVI) reduces its sensitivity. Therefore, considering that no previous information is supposed to be gathered beforehand when analyzing the satellite images, NHI is the recommended version of the index. However, among other potential applications, NHIc could be used for identifying those fields that are at an advanced phenological stage by comparing it with NHI.

A large number of the misclassified samples (mainly among the second season) corresponded to samples at Zadoks codes between 55 and 65. Misclassification could be explained by the fact that the spike of the main stem of each individual plant emerges several days earlier than the tillers, thus making detection of the precise phenological stage difficult. This limitation also reduces the accuracy of Zadoks characterization when phenology needs to be assessed manually during heading stage from specific points in the field. Therefore, higher variability was observed during this transition period, because some tillers reached full heading (Zadoks code 59) while others were beginning to spike (Zadoks code 50).

3.3. Analysis of broadband suitability

Taking into consideration the spectral response of the nine broadband ALI bands, the spectral ground measurements acquired at the experimental plots were resampled to ALI BER as previously described. Using the BER calculated for bands 6 and 7 as well as bands 4 and 5, NHI and NHIc were calculated as follows,

$$\mathrm{NHI} = \frac{B_6 - B_7}{B_6 + B_7} \tag{3}$$

$$\mathrm{NHIc} = \frac{\{(B_6 - B_7)(B_5 + B_4)\}}{\{(B_6 + B_7)(B_5 - B_4)\}} \tag{4}$$

where B_4: 0.63–0.69 μm; B_5: 0.775–0.805 μm; B_6: 0.845–0.89 μm; B_7: 1.2–1.3 μm. Band 6 was selected as the 1.1 μm surrogate since it showed the greatest correlation to ground reflectance measurements at 1.1 μm (r = 0.99).

Similar to narrow band data, misclassification was mostly ascribed to senescing plant samples, and could be improved using NHIc instead of NHI. However, this improvement was less pronounced than the one observed when using narrow band data (Table 1B). This might be explained by the smoothing that occurs by resampling the data to BER, reducing the variation of reflectance values between the two considered wavelengths.

3.4. Validation

3.4.1. Ground-level measurements

Applying the heading index in commercial farm fields resulted in levels of accuracy that were similar to levels observed

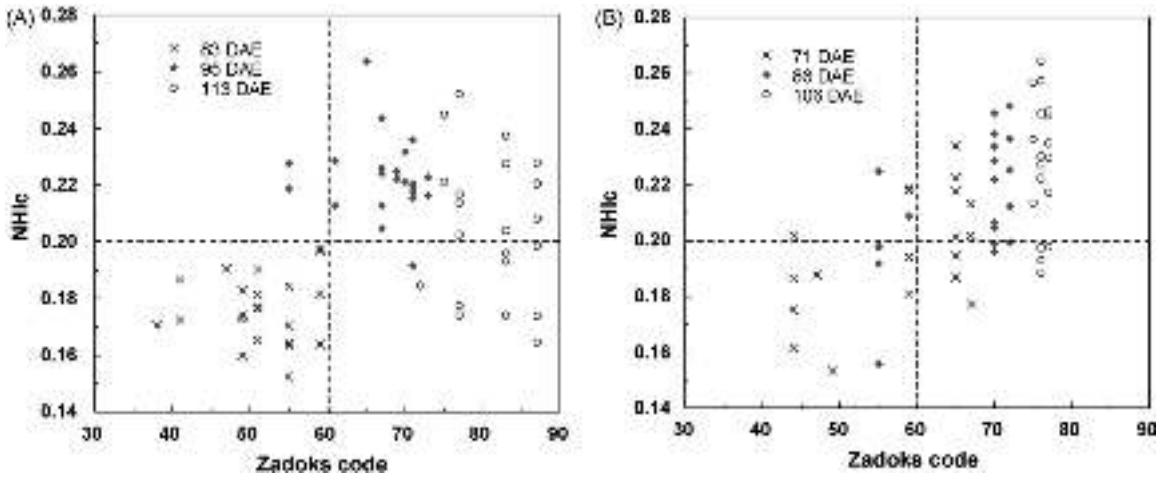

Fig. 4. Scatterplots of NHIc vs. Zadoks code using narrow bands spectral measurements. (A) 2004/2005 growing season; (B) 2005/2006 growing season. Dotted lines indicate the NHIc and Zadoks thresholds.

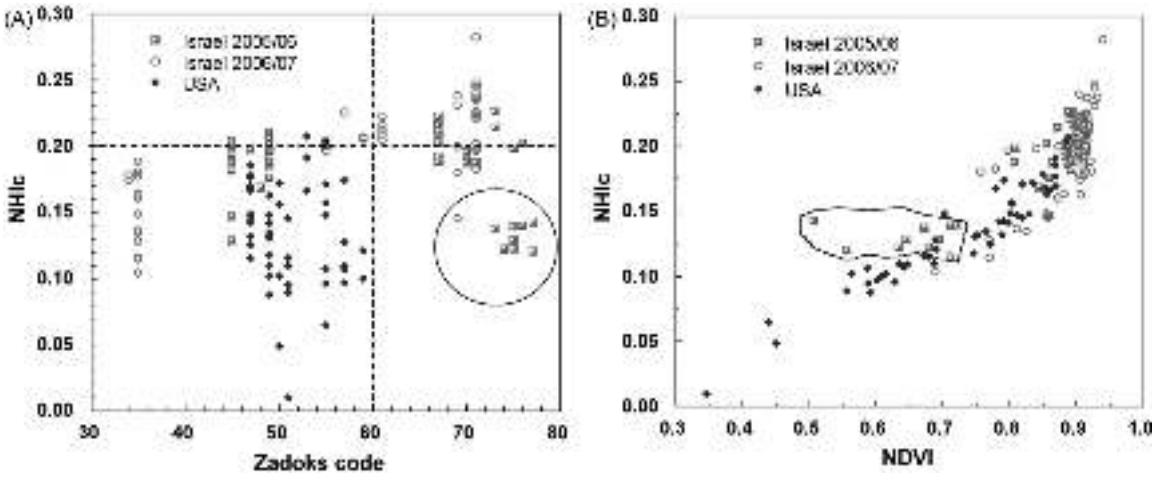

Fig. 5. Narrow band NHIc validation using field spectral measurements on commercial fields. (A) Scatterplot of NHIc vs. Zadoks code; (B) scatterplot of NHIc vs. NDVI. Israeli 2005/2006 samples marked by a circle correspond to the same samples in both figures.

in the experimental sites, showing that the narrow band and broad band version performed similarly in these commercial conditions too (Table 1). In addition, the validation results from the 2006/2007 season were better than those from the 2005/2006 season. Lower classification accuracy in 2005/2006 might be explained by some measurements that were taken at more advanced growth stages (Zadoks up to 77) vs. measurements that were acquired at earlier growth stages (Zadoks up to 71) in the 2006/2007 growing season. The adverse effect of senescing samples on classification accuracy is evident in Fig. 5A, where it can be seen that almost half of the misclassified samples were in an advanced development stage of grain-filling (Zadoks ~75). In contrast, samples collected at earlier development stages in the United States (Zadoks ~50–60) resulted in 96% classification accuracy. In comparison to the rest of the dataset, samples collected at more advanced growth stages appeared to have a lower canopy density (indicated by lower NDVI values), suggesting that the ability of NHI to accurately detect heading decreases with decreasing biomass (Fig. 5B). Lack of accuracy at low NDVI can be explained by the small difference observed between reflectance at 1.2 and 1.1 μm of those samples with low NDVI thus limiting the application of NHI to conditions where the biomass development is above optimum. Based on the analyzed data, optimum biomass conditions represented by NDVI values above 0.7, assures a good response of the NHI for the advanced development stage (Zadoks above 75).

3.4.2. Remote sensing of commercial fields—ALI satellite image

Different growth stages were observed within the fields depicted on the ALI image. As mentioned, the precipitation regime of the study area is characterized by high interannual and spatial variability. During the 2006/2007 season, germination started in November south of Kibbutz Saad and late December for the remainder of the study area due to differences in timing of germination triggering rainfall events. Therefore, a wide range of phenological stages was observed by the time the ALI image was acquired.

Applying the previously defined index thresholds to the data extracted from ALI imagery, resulted in a classification accuracy that was similar to that obtained for ground spectral data. The relationship between Zadoks code and NHI or NHIc is presented in Fig. 6 for 101 fields with NDVI greater than 0.7 calculated from the ALI image. This NDVI threshold value was suitable for these local conditions, but should be re-evaluated for other geographic locations. Considering these fields, the misclassification error increased from about 23–25% using field spectral data (Table 1), to 30 and 33% if using the previously defined thresholds of NHI and NHIc, respectively (Fig. 6). The greater error associated with satellite image data is likely due to the bidirectional reflectance

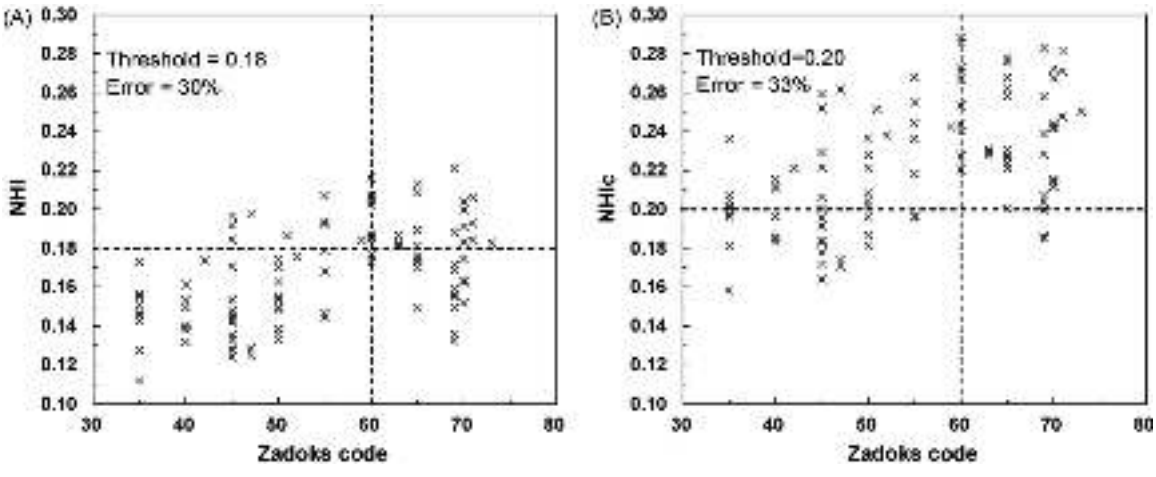

Fig. 6. Relationship between Zadoks code and heading indices of the commercial fields (ALI image February 25, 2007). (A) NHI; (B) NHIc. One hundred and one samples with NDVI higher than 0.7, out of 158 total samples, were considered.

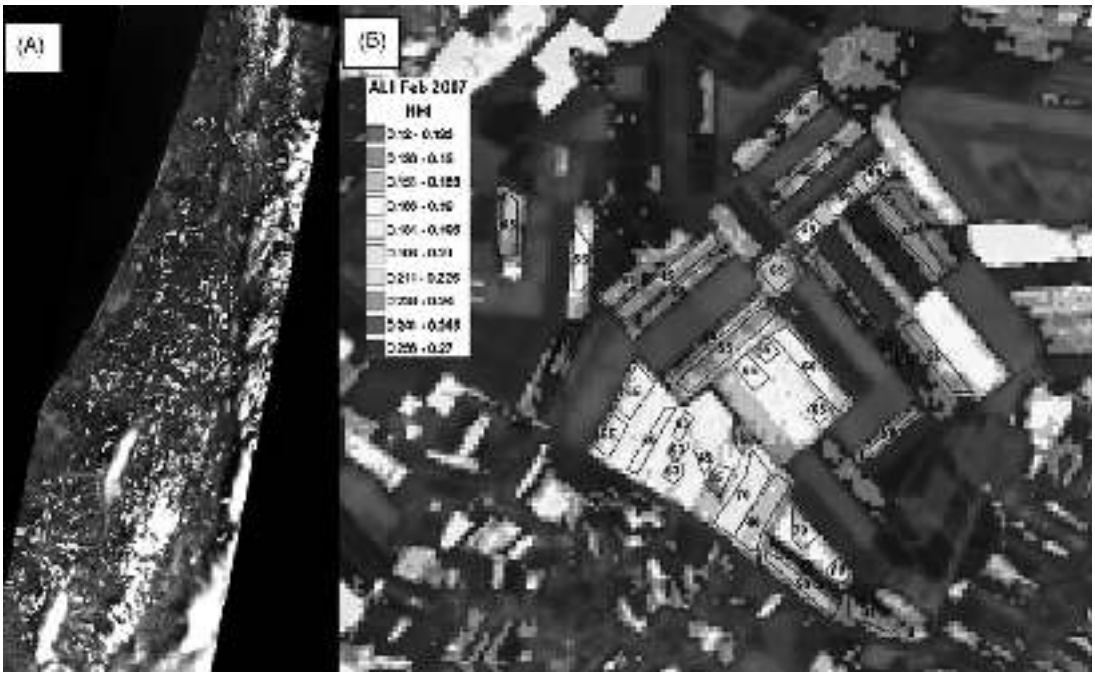

Fig. 7. NHI superimposed to the northwestern Negev, Israel true color ALI image collected in February 2007. Blue frame insert from Saad (right side) shows several fields with their respective Zadoks code. Areas with no NHI values were out of range, as other than wheat covered the area.

distribution function (BRDF), which has been demonstrated to negatively affect very stable vegetation indices as NDVI (Feingersh et al., 2005). Despite similar accuracy of both indices, as most of the NHIc misclassified samples correspond to samples at heading, makes the NHI more reliable alternative for the Heading-DSS.

Since the NHI generated better results for broadband data, it was superimposed over the complete true color ALI image of the northwestern Negev (Fig. 7). Looking at Fig. 7A it can be seen that there is a slight south-north trend of colors from light blue to red, indicating faster crop development in the south. This trend is due to the effect of rain on germination. Fig. 7B shows an example of one of the analyzed areas of the image, illustrating both the value of NHI in colors and the observed Zadoks code of each field following accurately the relationship presented in Fig. 6A. The possibility of identifying general patterns of crop development at large spatial scales represents another application for the novel NHI.

4. Conclusions

The main objective of this study was to propose an index able to identify the heading stage of wheat and validate its application to commercial farm fields. The proposed NHI was able to identify the onset of heading with a classification accuracy varying between 53 and 83%; the accuracy was strongly affected by the season and whether narrow (5 nm) or broad spectral bands were used. The classification accuracy for mapping the onset of heading of wheat was similar for ground based and ALI satellite imagery in commercial farm fields in Israel and the United States. These results suggest that the NHI is suited for identifying the onset of heading throughout wheat-growing areas and thus may indirectly improve remote predictions of crop conditions, and can be incorporated into decision support systems. Further research is needed to evaluate specific effects of variations in soil background, LAI, and BRDF on NHI.

Acknowledgements

This research was supported by Research Grant Award No. IS-3721-05R from BARD, The United States-Israel Binational Agricultural Research and Development Fund; the Chief Scientist of the Israeli Ministry of Agriculture, and the Israeli Ministry of Science, Culture, and Sport. The authors thank Silvia Asido from Gilat Research Center for her invaluable help in the field and laboratory. We also thank the Albert Katz International School for Desert Studies and the Israel Ministry of Immigration Absorption for granting a fellowship for the research period. Finally, we thank the staff and students of The Remote Sensing Laboratory at Sede-Boker for their constant help and support.

References

Acevedo, E., Silva, P., Silva, H., 2002. Wheat growth and physiology. In: Curtis, B.C., Rajaram, S., Gómez Macpherson, H. (Eds.), Bread Wheat: Improvement and Production. FAO, Rome, Italy, pp. 39–70.

Arnott, D., Pervan, G., 2005. A critical analysis of decision support systems research. J. Inform. Technol. 20, 67–87.

Bonfil, D.J., Karnieli, A., Raz, M., Mufradi, I., Asido, S., Egozi, H., Hoffman, A., Schmilovitch, Z., 2004a. Decision support system for improving wheat grain quality in the Mediterranean area of Israel. Field Crops Res. 89, 153–163.

Bonfil, D.J., Mufradi, I., Asido, S., 2004b. Decision support system for improving wheat quality in semi-arid regions. In: Mulla, D.J. (Ed.), 7th International Conference on Precision Agriculture and Other Precision Resources Management. ASA-CSSA-SSSA, Madison, WI, CD-ROM.

Bonfil, D.J., Mufradi, I., Klitman, S., Asido, S., 1999. Wheat grain yield and soil profile water distribution in a no-till arid environment. Agron. J. 91, 368–373.

Chavez, P.S., 1996. Image-based atmospheric corrections revisited and improved. Photgram. Eng. Rem. Sens. 62, 1025–1036.

Eitel, J.U.H., Gessler, P.E., Smith, A.M.S., Robberecht, R., 2006. Suitability of existing and novel spectral indices to remotely detect water stress in *Populus* spp. Forest Ecol. Manage. 229, 170–182.

Eitel, J.U.H., Long, D.S., Gessler, P.E., Smith, A.M.S., 2007. Using in-situ measurements to evaluate the new RapidEye satellite series for prediction of wheat nitrogen status. Int. J. Remote Sens. 28, 4183–4190.

Eom, S., Kim, E., 2006. A survey of decision support system applications (1995–2001). J. Operat. Res. Soc. 57, 1264–1278.

Feingersh, T., Dorigo, W., Richter, R., Ben-Dor, E., 2005. A new model-driven correction factor for BRDF effects in HRS data. In: Zagajewski, B., Sobczak, M. (Eds.), Proc. 4th EARSeL Workshop on Imaging Spectroscopy, Warsaw, Poland, pp. 565–576.

Fischer, A., 1994. A model for the seasonal variations of vegetation indices in coarse resolution data and its inversion to extract crop parameters. Remote Sens. Environ. 48, 220–230.

Flowers, M., Weisz, R., Heiniger, R., 2001. Remote sensing of winter wheat tiller density for early nitrogen application decisions. Agron. J. 93, 783–789.

Gao, B.C., 1996. NDWI—a normalized difference water index for remote sensing of vegetation liquid water from space. Remote Sens. Environ. 58, 257–266.
Gitelson, A.A., Kaufman, Y.J., Merzlyak, M.N., 1996. Use of a green channel in remote sensing of global vegetation from EOS-MODIS. Remote Sens. Environ. 58, 289–298.
Haboudane, D., Miller, J.R., Pattey, E., Zarco-Tejada, P.J., Strachan, I.B., 2004. Hyperspectral vegetation indices and novel algorithms for predicting green LAI of crop canopies: modeling and validation in the context of precision agriculture. Remote Sens. Environ. 90, 337–352.
Jensen, J.R., 2000. Remote Sensing of the Environment—An Earth Resource Perspective. Prentice-Hall Inc., Upper Saddle River, NJ.
Kobayashi, T., Kanda, E., Kitada, K., Ishiguro, K., Torigoe, Y., 2001. Detection of rice panicle blast with multispectral radiometer and the potential of using airborne multispectral scanners. Phytopathology 91, 316–323.
Lillesand, T.M., Kiefer, R.W., 2000. Remote Sensing and Image Interpretation. Wiley, New York.
Long, D.S., Engel, R.E., Carlson, G.R., 2000. Method for precision nitrogen management in spring wheat. II. Implementation. Prec. Agric. 2, 25–38.
Malley, D.F., Martin, P.D., Ben-Dor, E., 2004. Application in analysis of soils. In: Roberts, C.A., Workman, J., Reeves, J.B. (Eds.), Near-infrared Spectroscopy in Agriculture. ASA-CSSA-SSSA, pp. 729–784.
McBratney, A., Whelan, B., Ancev, T., Bouma, J., 2005. Future directions of precision agriculture. Prec. Agric. 6, 7–23.
Pal, B.P., 1966. Wheat. Indian Council of Agricultural Research, New Delhi.
Peñuelas, J., Gamon, J.A., Griffin, K.L., Field, C.B., 1993. Assessing community type, plant biomass, pigment composition, and photosynthetic efficiency of aquatic vegetation from spectral reflectance. Remote Sens. Environ. 46, 110–118.
Pimstein, A., Karnieli, A., Bonfil, D.J., 2007. Monitoring of wheat and maize crops based on ground spectral measurements and multivariate data analysis. J. Appl. Remote Sens. 1, 013530 (16 pages).
Pu, R., Ge, S., Kelly, N.M., Gong, P., 2003. Spectral absorption features as indicators of water status in coast live oak (*Quercus agrifolia*) leaves. Int. J. Remote Sens. 24, 1799–1810.
Rollin, E.M., Milton, E.J., 1998. Processing of high spectral resolution reflectance data for the retrieval of canopy water content information. Remote Sens. Environ. 65, 86–92.
Sakamoto, T., Yokozawa, M., Toritani, H., Shibayama, M., Ishitsuka, N., Ohno, H., 2005. A crop phenology detection method using time-series MODIS data. Remote Sens. Environ. 96, 366–374.
Salisbury, F.B., Ross, C.W., 1994. Fisiología Vegetal. Grupo editorial Iberoamericana, México.
Sims, D.A., Gamon, J.A., 2003. Estimation of vegetation water content and photosynthetic tissue area from spectral reflectance: a comparison of indices based on liquid water and chlorophyll absorption features. Remote Sens. Environ. 84, 526–537.
Viña, A., Gitelson, A.A., Rundquist, D.C., Keydan, G., Leavitt, B., Schepers, J., 2004. Monitoring maize (*Zea mays* L.) phenology with remote sensing. Agron. J. 96, 1139–1147.
Zadoks, J.C., Chang, T.T., Konnzak, C.F., 1974. A decimal code for growth stages in cereals. Weed Res. 14, 415–421.
Zarco-Tejada, P.J., Rueda, C.A., Ustin, S.L., 2003. Water content estimation in vegetation with MODIS reflectance data and model inversion methods. Remote Sens. Environ. 85, 109–124.